

University of Manitoba

THE MAGNETIC PROPERTIES  
OF IRON-ZINC FERRITES

by

P. A. Dickof

in partial fulfillment of the  
requirements for the degree of

Master of Science

Department of Physics

August, 1978

THE MAGNETIC PROPERTIES  
OF IRON-ZINC FERRITES

BY

PETER ALEXANDER DICKOF

A dissertation submitted to the Faculty of Graduate Studies of  
the University of Manitoba in partial fulfillment of the requirements  
of the degree of

MASTER OF SCIENCE

© 1978

Permission has been granted to the LIBRARY OF THE UNIVER-  
SITY OF MANITOBA to lend or sell copies of this dissertation, to  
the NATIONAL LIBRARY OF CANADA to microfilm this  
dissertation and to lend or sell copies of the film, and UNIVERSITY  
MICROFILMS to publish an abstract of this dissertation.

The author reserves other publication rights, and neither the  
dissertation nor extensive extracts from it may be printed or other-  
wise reproduced without the author's written permission.

## ABSTRACT

Experimental studies of the magnetic properties of mixed Fe-Zn ferrites of the form  $Zn_xFe_{3-x}O_4$  are presented. Magnetization measurements were performed as a function of temperature, field, and composition. The value of the moments on different sites of the compound was determined. Mössbauer measurements were taken for various temperatures and fields in order to obtain the temperature and field dependence of the canting angle and hyperfine fields. Relaxation effects were observed for  $x = 0.8$  well below the ordering temperature. These effects were found to be suppressed in a magnetic field.

A modified version of the localized canting model which considers second and third nearest neighbour interactions for some cases was developed. This model was used with the Mössbauer data to provide a fit of the spin structure to the bulk magnetic properties of the material.

## ACKNOWLEDGEMENTS

I would like to thank Dr. A. H. Morrish for his supervision of this thesis and Dr. P. J. Schurer for his active and invaluable involvement in the research. In addition, I would like to express my gratitude to Dr. C. M. Srivastava for the generous loan of the samples used in this investigation. Thank you also to Ms. J. S. Vaisey for editing and Mrs. R. A. Bobie for typing this thesis.

## TABLE OF CONTENTS

	<u>Page</u>
Abstract	i
Acknowledgements	ii
Table of Contents	iii
List of Figures	v
List of Tables	viii
Chapter 1 Introduction	1
References	6
Chapter 2 Theory	8
2.1 Ferrimagnetism in ferrites	8
2.2 Model revisions	14
2.3 Mössbauer effect	16
2.4 Relaxation effects.	22
References	24
Chapter 3 Magnetization Measurements	25
3.1 Equipment	25
3.2 Measurements	27
3.3 Results	28
References	38
Chapter 4 Mössbauer Measurements	39
4.1 Experimental techniques	39
4.2 Results at 4.2K	43
4.3 Results above 4.2K	58
References	72

	<u>Page</u>
Chapter 5 Discussion	73
5.1 Magnetization as a function of composition at 4.2K	73
5.2 The 0k0e canting angles and high field susceptibility at 4.2K	82
5.3 Magnetization above 4.2K	84
References	89
Chapter 6 Conclusions	90
Appendix A Calculation of multiple reversal probabilities.	91
Appendix B Comparison of measured $x = 0.8$ moments with moments calculated wusing free ion moments and fitted ion moments.	99
Appendix C. Comparison of the fit to the data provided by various models of the spin structure.	101

## LIST OF FIGURES

	<u>Page</u>
1.1 Lattice parameter as a function of Zn concentration.	4
2.1a Central B-site iron ion in a spinel structure surrounded by the six nearest oxygen ions and the six nearest A-site metal ions.	9
2.1b Central B-site iron ion in a spinel structure surrounded by the six nearest oxygen ions and the six nearest B-site iron ions.	9
2.2 Ferrimagnetic spin structure of $Fe_3O_4$ .	11
2.3a Angular relationship between magnetic and hyperfine fields.	11
2.3b Angular relationship of spins in fields of fig. 2.3a.	11
2.4 Hyperfine field splitting for an axially symmetric electric field gradient tensor with symmetry axis parallel to H.	21
2.5 Hyperfine spectrum for an axially symmetric electric field gradient tensor with symmetry axis parallel to H.	21
3.1 Magnetometer coil system for use with superconducting solenoid.	26
3.2 Plexiglass coil former.	25
3.3 Magnetization of $Zn_x Fe_{3-x} O_4$ versus applied field for $x = 0.0, 0.2, 0.4, 0.6$ and $0.8$ .	29
3.4 Magnetization versus Zn concentration.	31
3.5 Spontaneous magnetization versus temperature.	32
3.6 Magnetization versus temperature for $Zn_{0.6} Fe_{2.4} O_4$ .	34
3.7 Magnetization versus temperature for $Zn_{0.8} Fe_{2.2} O_4$ .	35
3.8 Magnetization versus applied field for $Zn_{0.8} Fe_{2.2} O_4$ , $T=4.2K, 40K, 37$	
4.1 Hyperfine fields and canting angle.	42

	<u>Page</u>
4.2 Mössbauer spectrum of $x = 0.0$ at 4.2K, 0kOe.	45
4.3 Mössbauer spectrum of $x = 0.2$ at 4.2K, 0kOe.	45
4.4 Mössbauer spectrum of $x = 0.4$ at 4.2K, 0kOe.	46
4.5 Mössbauer spectrum of $x = 0.4$ at 4.2K, 10kOe.	46
4.6 Mössbauer spectrum of $x = 0.4$ at 4.2K, 50kOe.	47
4.7 Mössbauer spectrum of $x = 0.6$ at 4.2K, 0kOe.	47
4.8 Mössbauer spectrum of $x = 0.6$ at 4.2K, 10kOe.	51
4.9 Mössbauer spectrum of $x = 0.6$ at 4.2K, 25kOe.	51
4.10 Mössbauer spectrum of $x = 0.6$ at 4.2K, 50kOe.	52
4.11 Mössbauer spectrum of $x = 0.8$ at 4.2K, 0kOe.	52
4.12 Mössbauer spectrum of $x = 0.8$ at 4.2K, 8.6kOe.	56
4.13 Mössbauer spectrum of $x = 0.8$ at 4.2K, 15.4kOe.	56
4.14 Mössbauer spectrum of $x = 0.8$ at 4.2K, 30kOe.	57
4.15 Mössbauer spectrum of $x = 0.8$ at 4.2K, 50kOe.	57
4.16 Mössbauer spectrum of $x = 0.2$ at 85K, 0kOe.	63
4.17 Mössbauer spectrum of $x = 0.4$ at 85K, 0kOe.	63
4.18 Mössbauer spectrum of $x = 0.6$ at 20K, 0kOe.	65
4.19 Mössbauer spectrum of $x = 0.6$ at 32K, 10kOe.	65
4.20 Mössbauer spectrum of $x = 0.6$ at 32K, 50kOe.	66
4.21 Mössbauer spectrum of $x = 0.6$ at 85K, 0kOe.	66
4.22 Mössbauer spectrum of $x = 0.8$ at 11.6K, 0kOe.	67
4.23 Mössbauer spectrum of $x = 0.8$ at 20K, 0kOe.	67
4.24 Mössbauer spectrum of $x = 0.8$ at 20K, 30kOe.	68
4.25 Mössbauer spectrum of $x = 0.8$ at 20K, 50kOe.	68
4.26 Mössbauer spectrum of $x = 0.8$ at 40K, 0kOe.	69
4.27 Mössbauer spectrum of $x = 0.8$ at 40K, 30kOe.	69
4.28 Mössbauer spectrum of $x = 0.8$ at 40K, 50kOe.	70



	<u>Page</u>
5.1 Reduced magnetization versus Zn concentration.	74
5.2 Spin structure of $Zn_xFe_{3-x}O_4$ for $x = 0.6, 0.8$ .	83
C.1 Mössbauer spectrum of $x = 0.8$ at 4.2K, 50kOe.	103
C.2 Mössbauer spectrum of $x = 0.8$ at 40K, 50kOe.	103

LIST OF TABLES

	<u>Page</u>
2.1. Multiple reversal probabilities for $x = 0.6$ and $x = 0.8$ .	15
2.2. Probabilities for reversed and unreversed spins in samples with $x = 0.6$ and $x = 0.8$ .	15
3.1. Curie temperatures derived from magnetization measurements.	33
3.2. The average high field susceptibility above 10kOe for $x = 0.8$ at 4.2K and 40K.	36
4.1. Mössbauer data for $x = 0.0$ and 0.2 at 4.2K.	49
4.2. Mössbauer data for $x = 0.4$ at 4.2K.	50
4.3. Definition of B site subspectra.	53
4.4. Mössbauer data for $x = 0.6$ at 4.2K.	54
4.5. Mössbauer data for $x = 0.8$ at 4.2K.	54
4.6. Mössbauer data for $x = 0.2$ and $x = 0.4$ above 4.2K.	59
4.7. Mössbauer data for $x = 0.6$ above 4.2K.	60
4.8. Mössbauer data for $x = 0.8$ above 4.2K.	61
5.1. Fitted values of moments.	76
5.2. Internal hyperfine fields for $x = 0.0$ and 0.2 at 4.2K.	77
5.3. Internal hyperfine fields for $x = 0.4$ at 4.2K.	77
5.4. Magnetic moment of $x = 0.4$ at 4.2K as measured by magnetization and calculated from Mössbauer results.	78
5.5. Internal hyperfine fields and canting angles for $x = 0.6$ at 4.2K.	80
5.6. Magnetic moment of $x = 0.6$ at 4.2K as measured by magnetization and calculated from Mössbauer results.	79
5.7. Internal hyperfine fields and canting angles for $x = 0.8$ at 4.2K.	79
5.8. Magnetic moment of $x = 0.8$ at 4.2K as measured by magnetization and calculated from Mössbauer results.	81

	<u>Page</u>
5.9. Canting angles calculated to fit $H = 0$ , $T = 4.2\text{K}$ magnetization data.	82
5.10. Average canting angles estimated from $4.2\text{K}$ high field susceptibility and from $H = 0\text{kOe}$ , $T = 4.2\text{K}$ magnetization fit.	84
5.11. Internal hyperfine fields for $x = 0.2$ and $0.4$ at $85\text{K}$ .	85
5.12. Internal hyperfine fields for $x = 0.6$ above $4.2\text{K}$ .	85
5.13. Magnetic moment of $x = 0.6$ above $4.2\text{K}$ as measured by magnetization and calculated from Mössbauer results.	86
5.14. Internal hyperfine fields for $x = 0.8$ above $4.2\text{K}$ .	85
5.15. Magnetic moment of $x = 0.8$ above $4.2\text{K}$ as measured by magnetization and calculated from Mössbauer results.	86
A.1. Probability for Zn A-site substitution in one group.	93
A.2. Probability for some possible Zn A-site substitutions in two groups.	94
A.3. Probability for a B-site spin to have $m$ Zn A-site neighbours for a concentration of $x$ .	95
A.4. Multiple reversal probabilities for $x = 0.6$ up to double reversal.	92
A.5. Multiple reversal probabilities for $x = 0.8$ up to double reversal.	96
A.6. Multiple reversal probabilities for $x = 0.6$ and $0.8$	97
A.7. Probabilities for various differentiated B sites.	98
B.1. Measured magnetization values, free ion calculated values and fitted ion calculated values for the moment of $x = 0.8$ at various temperatures and fields.	100

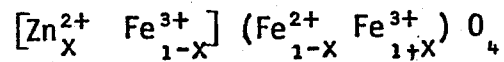
CHAPTER 11-1. INTRODUCTION

Mixed Zn ferrites of the type  $Zn_x M_{3-x} O_4$  where M is a magnetic ion have been the subject of numerous investigations in the past, especially with regard to their magnetic properties<sup>1,2</sup>. The metallic ions occupy the tetrahedral A or octahedral B sites in the spinel crystal structure. The Zn ions preferentially occupy the A sites because of their tendency to form covalent bonds involving  $sp^3$  orbitals. The magnetic moments at  $x = 0$  on the A sites are aligned anti-parallel while those on the more numerous B sites are parallel to the magnetization direction. Therefore, the substitution of diamagnetic Zn ions for the M ions on the A sublattice is expected to result in an increase in the magnetic moment of the sample at 0K proportional to the amount of substitution. Such is indeed the case in the region where  $x < 0.5$ , although the increase is less than expected if free ion magnetic moments for the M ions are assumed. At higher Zn concentrations, i.e.,  $x \gtrsim 0.5$ , the moment begins to decrease and for  $x = 1.0$ , an antiferromagnetic structure is observed.<sup>3</sup> Several explanations have been offered for the behaviour of the magnetization for  $x \gtrsim 0.5$ ,<sup>4,5,6</sup> but spin canting has been determined to be primarily responsible. The canting angles have been measured for several systems using

the neutron diffraction<sup>7</sup> or the Mössbauer effect techniques.<sup>8,12</sup> By using the measured values of the canting angles it is possible in principle to fit quantitatively the magnetization results. No such work has yet been done. Magnetization results and Mössbauer results have primarily been determined for different samples, and at differing temperatures and fields. A study to fit quantitatively the canting angles should allow a decision on whether or not the spin canting is solely responsible for the magnetization behaviour. It should be noted that a Mössbauer study can only give information about canting of the Fe magnetic moments. Therefore, the only mixed Zn system for which a correlation between magnetization and Mössbauer effect measurements is possible is the  $Zn_x Fe_{3-x} O_4$  system.

Another interesting phenomenon in mixed Zn ferrites is the occurrence of relaxation effects in the Mössbauer spectra. This is usually explained as being caused by ionic spin flipping<sup>8,13</sup>; however, superparamagnetic clusters<sup>6</sup> and domain wall oscillations<sup>14,15</sup> have also been proposed. Frequently, one finds that the Curie temperatures, as measured by the Mössbauer effect, neutron diffraction, and magnetization measurements, differ from each other.<sup>16-23</sup> This is probably correlated with the relaxation phenomena in the high Zn region, and the measurement time for each technique.

The present study consists of magnetization and Mössbauer effect measurements for ferrites of the type



The system was first studied by Stuijts et al<sup>24</sup> for  $x \lesssim 0.7$ . As with other mixed Zn ferrites, the magnetization  $M$  was shown to increase with increasing  $x$  until  $x \approx 0.5$  after which it began to decrease. Also of interest was a peak in the magnetization versus temperature curve for  $x = 0.7$  at 40K. Similar peaks were also observed by Ishikawa<sup>6</sup> in the Ni-Zn system. This maximum has not yet been explained.

A more recent study has been published by Srivastava et al<sup>14,15</sup> on samples with  $x = 0.0, 0.2, 0.4, 0.6,$  and  $0.8$ . Their work showed magnetization results from 77K and 300K, and permeability spectra at 300K. The primary focus of their study was the relaxation phenomena which were found to occur well below the Curie temperature at the higher Zn concentrations ( $x > 0.5$ ). These samples were prepared in a way similar to those of Stuijts et al<sup>24</sup>, and were generously made available to us for the present study. X-ray diffraction techniques showed the samples to be free of impurity phases. The lattice parameters were measured using a Debye-Scherrer powder diffraction camera, and are plotted as a function of Zn concentration in fig. 1.1. The linear increase in lattice

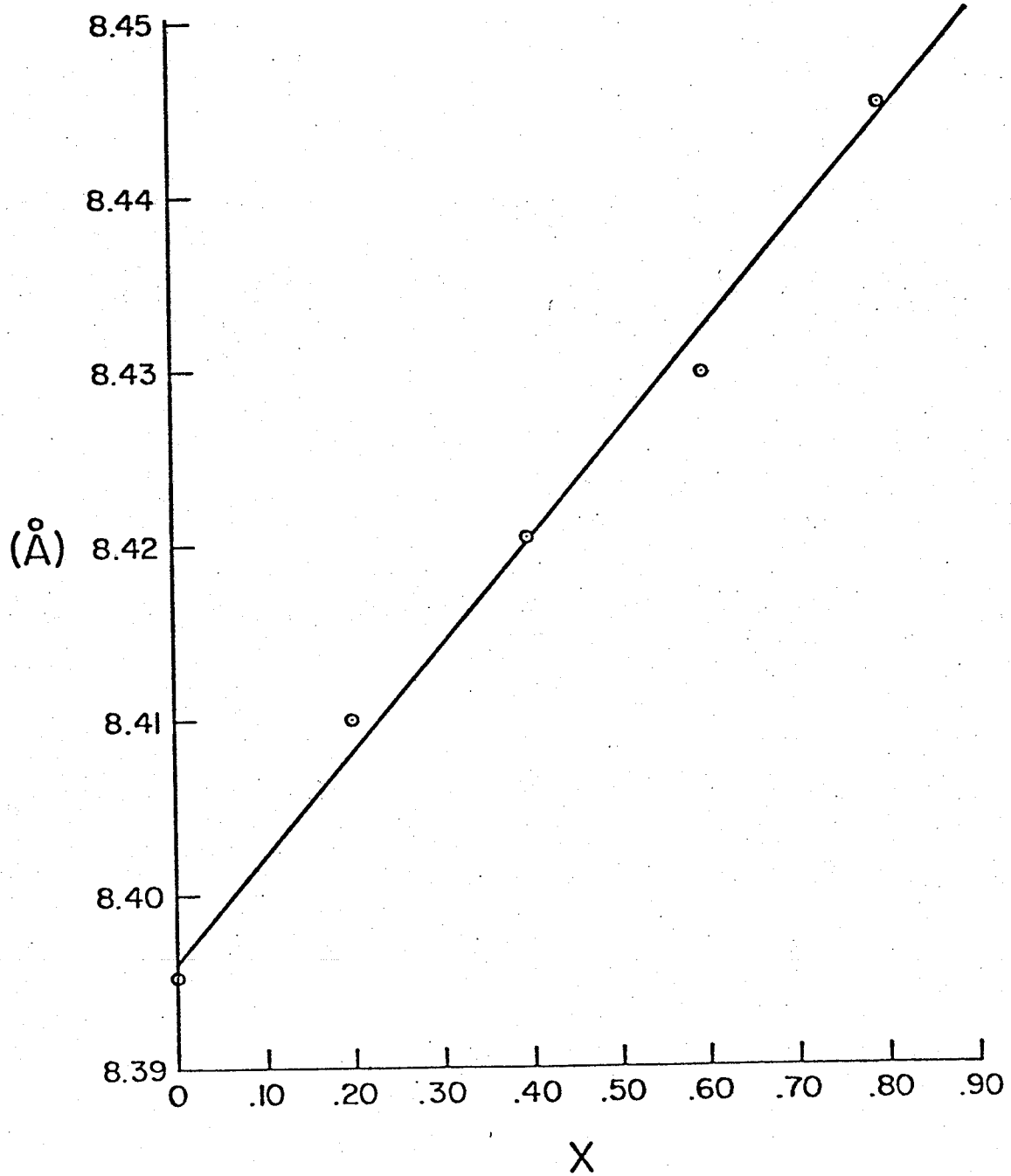


Fig. 1.1 Lattice parameter as a function of Zn concentration.

parameter with Zn concentration derives from the larger size of the  $\text{Zn}^{2+}$  ions as compared to the  $\text{Fe}^{3+}$  ions. The high angle lines were not broadened, indicating that the samples had a uniform Zn distribution. This thesis will compare our measured magnetization values with those calculated from the microscopic spin structure as determined from our Mössbauer study.



REFERENCES, INTRODUCTION

1. J. Smit and H. P. J. Wijn, Ferrites (Wiley, New York 1959).
2. Y. Hoshino et al (Eds.) Ferrites, Proceedings of the International Conference 1970 (Univ. Park Press, Baltimore London, Tokyo, 1971).
3. U. König et al, Sol. Stat. Comm., 8 (1970) 759.
4. M. A. Gilleo, Phys. Chem. Solids, 13 (1960) 33.
5. I. Nowik, J. Appl. Phys., 40 (1969) 872.
6. Y. Ishikawa, J. Phys. Soc. Japan, 17 (1962) 1877.
7. N. S. Satya Murthy et al, Phys. Rev., 181 (1969) 969.
8. J. M. Daniels and A. Rosencwaig, Can. Journal Phys., 48 (1970) 381.
9. L. K. Leung et al, Phys. Rev. B, 8 (1973) 29.
10. A. H. Morrish and P. J. Schurer, Physica, 86-88B (1977) 921.
11. P. E. Clark and A. H. Morrish, Phys. Stat. Sol. (a), 19 (1973) 687.
12. A. H. Morrish and P. E. Clark, Phys. Rev. B, 11 (1975) 278.
13. P. K. Iyengar and S. C. Bhargava, Phys. Stat. Sol. (b), 53 (1972) 359.
14. C. M. Srivastava et al, Phys. Rev. B, 14 (1976) 2032.
15. C. M. Srivastava et al, Phys. Rev. B, 14 (1976) 2041.
16. H. Szydlowski et al, Phys. Stat. Sol. (a), 2 (1970) K37.
17. H. Szydlowski et al, Phys. Stat. Sol. (a), 3 (1970) 769.
18. J. G. Booth and J. Crangle, Proc. Phys. Soc. Lond., 79 (1962) 1271.

19. G. A. Petitt and D. W. Forrester, Phys. Rev. B, 4 (1971) 3912.
20. P. K. Iyengar and S. C. Bhargava, Phys. Stat. Sol. (b) 46 (1971) 117.
21. J. G. Booth, Proc. Phys. Soc. Lond., 79 (1962) 1271.
22. S. C. Bhargava, Phys. Stat. Sol. (b) 53 (1972) 359.
23. C. Guillard and H. Crevaux, Compt. Rend., 230 (1950) 1256.
24. A. L. Stuijts et al, Ferrites, Proceedings of the International Conference 1970, p.236.

## CHAPTER 2

### THEORY

#### 2-1. FERRIMAGNETISM IN FERRITES.

Ferrimagnets are ordered magnetic materials having two or more lattices antiferromagnetically aligned with a larger moment in one direction than the others. Ferrites, of which  $[\text{Fe}^{3+}] (\text{Fe}^{2+} \text{Fe}^{3+}) \text{O}_4$  is an example, are a class of ferrimagnetic metal oxides possessing a spinel structure. In this structure, metal ions occupy two different types of sites: A sites, indicated with brackets [ ]; and B sites, indicated with parentheses ( ). The A sites are tetrahedrally coordinated, and the B sites, of which there are twice as many occupied, are octahedrally coordinated as shown in figs. 2.1a and 2.1b.

The exchange interactions in the two lattices can be represented with 3 exchange parameters:  $J_{AB}$ , the intersublattice exchange parameter; and  $J_{BB}$  and  $J_{AA}$ , the intrasublattice exchange parameters. The molecular field for a spin on the  $i$ th lattice can then be written as

$$\vec{H}_i = \frac{2}{g\mu_B} (\vec{S}_j J_{ij} + \vec{S}_i J_{ii})$$

where  $\vec{S}_i$  and  $\vec{S}_j$  represent the sum of the 6 neighbouring moments on either lattice, i.e.:

$$\vec{S}_A = \frac{6\mu_A}{g\mu_B} \quad ; \quad \vec{S}_B = \frac{6\mu_B}{g\mu_B}$$

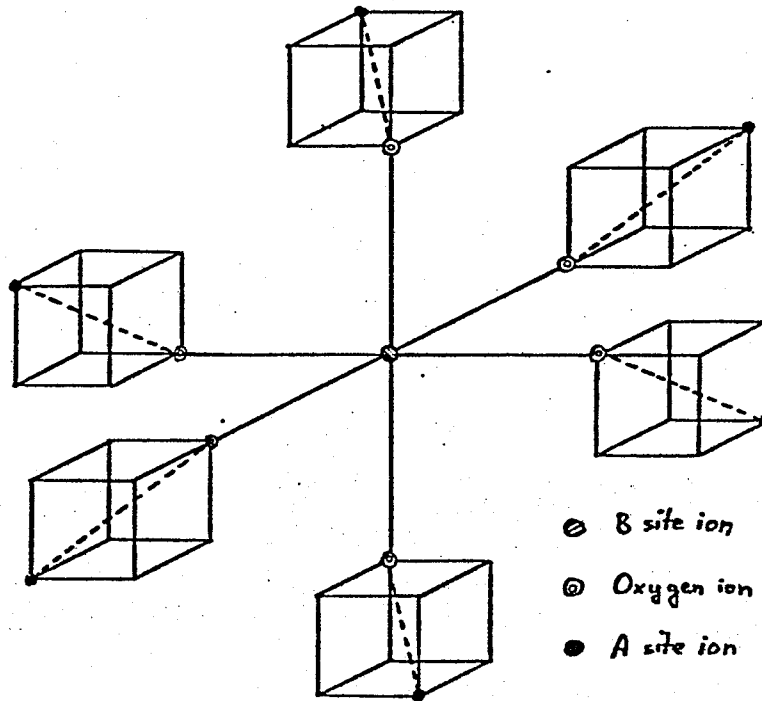


Fig. 2.1a Central B-site iron ion in a spinel structure surrounded by the six nearest oxygen ions and the six nearest A-site metal ions.

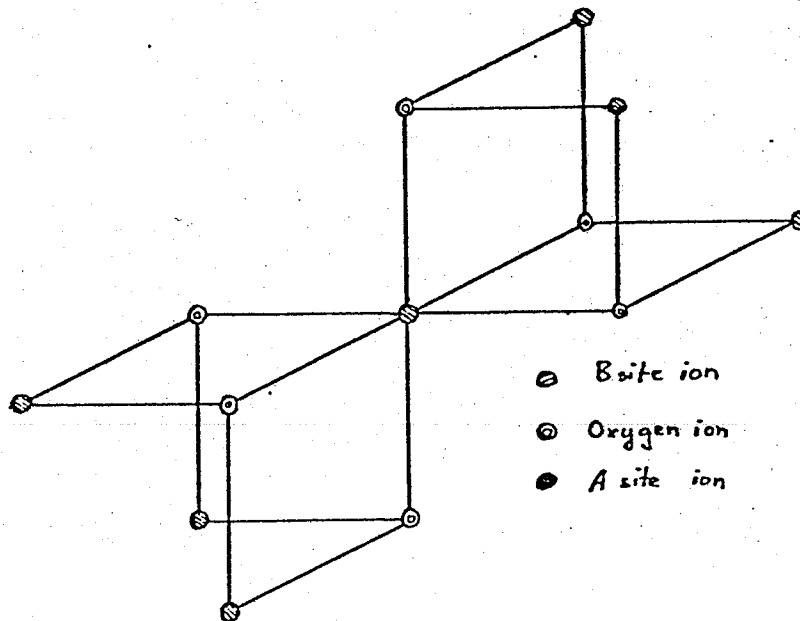


Fig. 2.1b Central B-site iron ion in a spinel structure surrounded by the six nearest oxygen ions and the six nearest B-site iron ions.

Here  $\mu_\alpha$  and  $\mu_\beta$  are the magnetic moments of spins on the A and B lattices respectively. From the chemical formula of the example above, and using the free ion magnetic moments of  $5\mu_B$  for  $\text{Fe}^{3+}$  ions and  $4\mu_B$  for  $\text{Fe}^{2+}$  ions, we get  $\mu_\alpha = 5\mu_B$  and  $\mu_\beta = 4.5\mu_B$ . As  $|J_{AB}| > |J_{BB}| > |J_{AA}|$ , and the exchange parameter  $J_{AB}$  is negative because of the antiferromagnetic nature of the superexchange interaction in ferrites, the two sublattices are arranged in an antiparallel fashion as shown in figure 2.2.

In  $[\text{Zn}_x^{2+} \text{Fe}_{1-x}^{3+}] (\text{Fe}_{1-x}^{2+} \text{Fe}_{1+x}^{3+})_4 \text{O}_4$ , diamagnetic  $\text{Zn}^{2+}$  ions are randomly substituted onto the A sublattice, resulting in a change in  $\vec{S}_A$  and  $\vec{S}_B$ , and in a breaking of exchange interactions. Geller et al<sup>1</sup> proposed that random canting occurred on the unsubstituted lattice under these conditions, on the basis of their experimental data. This proposal was mathematically developed by Rosencwaig<sup>2</sup>, and is outlined here.

Random substitution of diamagnetic ions is assumed on the A site, and some average canting angle  $\phi$ , with respect to the magnetization direction, is assumed for the B site. This allows us to write the local molecular field for a given B site ion called  $B_i$ , as

$$\vec{H}_i = \frac{2}{g\mu_B} \left( \vec{S}_A J_{AB} + \vec{S}_B J_{BB} \right) .$$

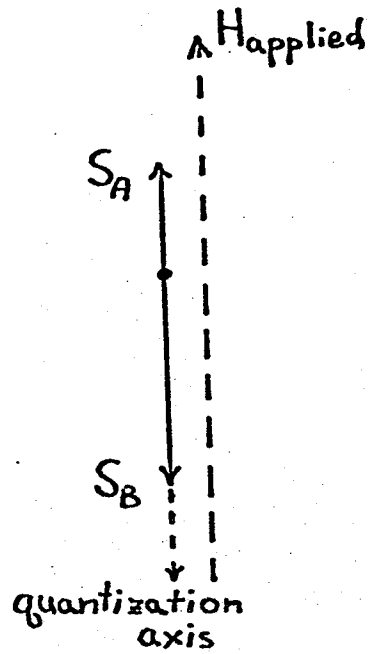


Fig. 2.2 Ferrimagnetic spin structure of  $\text{Fe}_3\text{O}_4$ .

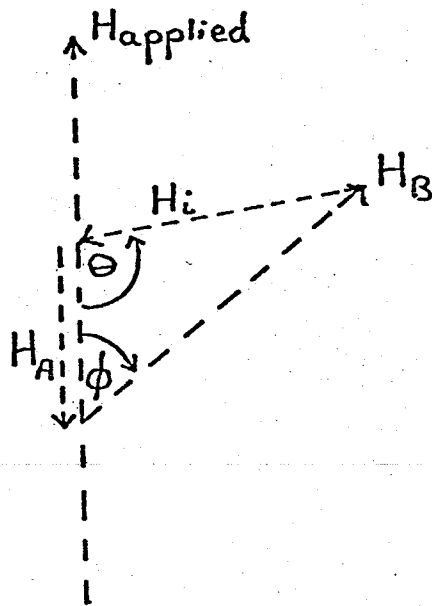


Fig. 2.3a Angular relationship between magnetic and hyperfine fields.

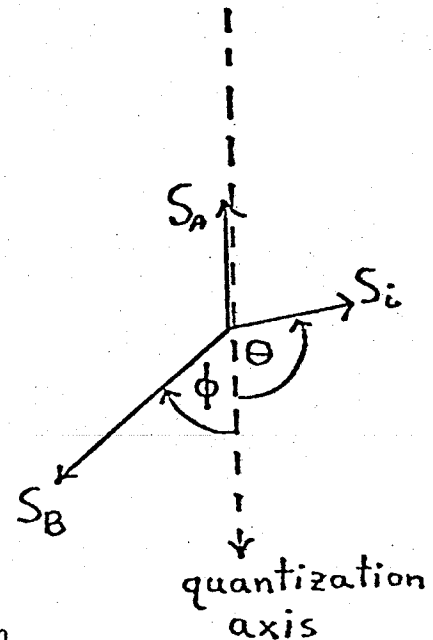


Fig. 2.3b Angular relationship of spins in fields of fig. 2.3a.

Since there is diamagnetic substitution on the A lattice, we may write

$$|\vec{S}_A| = \frac{(6-m)\mu_\alpha}{g\mu_B}$$

where  $m$  is the number of neighbouring A sites occupied by diamagnetic ions. Similarly, we have

$$|\vec{S}_B| = \frac{6\mu_B(x)}{g\mu_B},$$

where

$$\mu_B(x) = (1-x)\mu_B^{2+} + (1+x)\mu_B^{3+},$$

and  $\mu_B^{2+}$  and  $\mu_B^{3+}$  represent the moments of the B site  $\text{Fe}^{2+}$  and  $\text{Fe}^{3+}$  ions respectively. In fig. 2.3a,  $\vec{H}_i$  as well as the component terms  $\vec{H}_A$  and  $\vec{H}_B$  are shown. The resultant spin structure, with the moment  $S_i$  taking a canting angle of  $\theta$  with respect to the magnetization direction, is shown in fig. 2.3b. By using fig. 2.3a, and the formula for the local molecular field, we may write

$$\cos \theta = \frac{S_A - S_B \delta \cos \phi}{[S_A^2 + (S_B \delta)^2 + 2S_A S_B \cos \phi]^{\frac{1}{2}}}$$

where

$$\delta = \frac{J_{BB}}{J_{AB}}.$$

It is clear that  $\theta$  can take on any value between  $0^\circ$  and  $180^\circ$  depending on the value of the term  $S_A - S_B \delta \cos \phi$ . If

$S_A > S_B \delta \cos \phi$ , i.e., if the net intersublattice interaction on a spin is greater than the net intrasublattice interaction, then  $\theta$  will be smaller than the average canting angle  $\phi$ . If  $S_A < S_B \delta \cos \phi$ , then  $\theta$  will be larger than the average canting angle  $\phi$ , and if  $S_A = 0$ , then the  $B_i$  spin will be aligned antiparallel to the B sublattice and the magnetization direction.

In order to calculate any bulk properties of the mixed Zn ferrite, we must calculate the probability of a spin having  $m$  of its six A sites occupied by  $Zn^{2+}$  ions. This is determined by the binomial distribution:

$$P(x,m) = \binom{6}{m} x^{6-m} (1-x)^m$$

which allows us to write the O-K magnetic moment as

$$\mu(x, T=0) = 2 \sum_{m=0}^6 P(x,m) \cos [\theta(x,m)] \mu_B(x) - (1-x) \mu_\alpha$$

The first term indicates the decrease in moment due to random canting on the B sublattice, and the second represents the increase in moment due to diamagnetic substitution on the antiparallel A sublattice.

This model has been successfully applied to the substituted Yttrium Iron Garnets, and gives a qualitative agreement with the experimental data for Zn substituted ferrites. Neutron diffraction<sup>3</sup> and Mössbauer effect<sup>4</sup> data show canting angles in these systems for Zn substitution in excess of  $x \approx 0.5$ .



However, no quantitative correlation has been published as yet. Reasons for this include the facts that magnetization, neutron diffraction and Mössbauer results have largely come from different samples. Also, canting angles, as determined by the Mössbauer effect, have been measured in relatively large fields and not compared with magnetization results in the same field.

## 2.2 MODEL REVISIONS

The major flaw of the localized canting model is that only first nearest neighbour interactions are considered. In most cases, this is a justifiable approximation, but for cases in which there are spins having canting angles  $\theta > 90^\circ$ , a revision is required, considering second and even third nearest neighbour interactions.

Spins which have canting angles  $\theta > 90^\circ$  will be referred to as "reversed" spins. If all or nearly all of the B site neighbours of one of these reversed spins are themselves reversed, then that spin will have been reversed twice. Similarly, if all the neighbours to a reversed spin are themselves doubly reversed, that spin will have been triply reversed. Since  $|J_{AB}|$  is known to be much larger than  $|J_{BB}|$  we will assume that only those spins with all six nearest neighbour A sites occupied by Zn ions can be reversed. The probabilities for such multiple reversals occurring are higher than might at first be expected. This is because the B site nearest neighbours of a spin having six

Zn A site nearest neighbours each have three Zn A site nearest neighbours which are shared with the central spin. The remaining A site neighbours are shared among each other. The calculations for multiple reversal (single and double reversal for  $x = 0.6$  and single and triple reversal for  $x = 0.8$ ) are given in Appendix A, where the notation used in the following discussion is defined. The probabilities for multiple reversals are extremely small for all other cases. The results of these calculations are as shown in table 2.1.

TABLE 2.1

Multiple reversal probabilities for  $x = 0.6$  and  $x = 0.8$ .

Sample	Unreversed ( $B_0 - B_5$ )	Single Reversal $B_6$	Double Reversal $B_6$	Triple Reversal $B_6$
$x = 0.6$	0.95334	0.04274	0.00392	---
$x = 0.8$	0.73786	0.15219	0.08121	0.02874

This allows determination of the total number of spins reversed or unreversed with respect to the magnetization direction, as shown in table 2.2.

TABLE 2.2

Probabilities for reversed and unreversed spins in samples with  $x = 0.6$  and  $x = 0.8$ .

Sample	Unreversed ( $B_{05}$ )	Reversed ( $B_6$ )	Unreversed ( $B_6$ )
$x = 0.6$	0.95334	0.00392	0.04274
$x = 0.8$	0.73786	0.08121	0.18093

The bulk magnetic moment at  $T = 0$  K may now be written as

$$\mu(x, T=0) = \sum_{m=0}^5 \left\{ P(m, x) \cos[\theta(m, x)] + P(6', x) \cos[\theta(6', x)] \right. \\ \left. + P(6, x) \cos[\theta(6, x)] \right\} 2\mu_B - (1-x)\mu_\alpha$$

One would expect  $\theta(6, x)$  to be quite close to zero, since the only interaction that a  $B_6$  site has is with  $B_6'$  sites, each having the same canting angle with respect to the quantization axis. An average of the six  $B_6'$  spins, will therefore be of the form:

$$\bar{S}_6 = S \frac{\cos \theta}{6} \sum_{i=1}^6 \cos \psi_i \hat{x} + S \frac{\cos \theta}{6} \sum_{i=1}^6 \sin \psi_i \hat{y} + S \sin \theta \hat{z}$$

Since the spins will be randomly distributed over the azimuthal angle  $\psi_i$ , the first two terms will be close to zero.

This analysis will be used in Chapter 5 of this thesis to compare the Mössbauer and magnetization results.

## 2.3 MÖSSBAUER EFFECT

### General Theory

The energy difference for a given nuclear transition is a well defined quantity, but in general, the energy distribution of gamma rays emitted or absorbed in such a transition is quite broad due to the recoil of the nucleus involved. In solids however,